



Ultra-high energy neutrinos with IceCube

Aya Ishihara^{a,b}^afor the IceCube collaboration^bFaculty of Science, Chiba University, 1-33, Yayoi-cho, Inage-ku, Chiba-shi, Chiba, 263-8522 Japan

Abstract

We report on a search for ultra-high energy neutrinos with energy greater than 10^6 GeV using the data taken with the IceCube detector at the South Pole. The data was collected between June 2010 and May 2011 when 90% of the IceCube detector was in operation and from May 2011 to May 2012 which corresponds to the first physics run with the fully completed IceCube detector. Two signal neutrino candidate events are observed in the sample of 670.1 days of livetime over expected background rates of 0.06 events. These events are consistent with the cascade-like events induced by ν_e charged current or $\nu_{e,\mu,\tau}$ neutral current interaction within the IceCube detector volume. Preliminary p-values for a background-only hypothesis are 1.6×10^{-3} (2.9σ) without a prompt atmospheric neutrino contribution and 1.5×10^{-2} (2.2σ) with a default perturbative QCD-based prompt neutrino contribution.

Keywords: Astrophysical neutrinos, Ultra-high energy cosmic-rays, the GZK effect

1. Introduction

Neutrinos are important probes for exploring the high energy universe. Because of their unique nature, neutrinos are undeflected in the galactic or extra-galactic magnetic fields and unabsorbed in the photon-filled universe, and thus they may be the missing link between TeV gamma-rays and EeV cosmic-rays. Photons, which are the conventional messengers from the universe, are highly attenuated by cosmic microwave background in this energy range. Therefore, cosmic neutrinos at PeV energies or higher are of particular importance for the complete survey of the ultra-high energy universe.

Cosmic neutrinos are expected to be produced by interactions of high energy hadronic beams from cosmic accelerators with surrounding photons and/or matter. However, the neutrino flux produced in each source is highly uncertain. A way of detecting neutrinos from possible weak sources is the diffuse neutrino search. This is because superposition of fluxes from all the weak astrophysical neutrino sources could compose a detectable signal. Still, the expected astrophysical neutrino flux is so small that a huge target is required in order for neutrinos to interact and produce secondary

charged particles that can be detected through their Cherenkov emissions. With IceCube [1], the first cubic-kilometer scale neutrino detector is realized.

IceCube construction started in 2005 and was completed in December 2010. IceCube had been in operation with the partial detector configurations since 2005 until the beginning of the full configuration run. IceCube uses 2,800 m thick glacial ice as a Cherenkov medium. Cherenkov photons emitted from relativistic charged particles are detected by an array of Digital Optical Modules (DOMs) that amplify and digitally sample the high-speed pulses [3] from the enclosed photomultiplier tube (PMT) [2]. The cable assemblies, often called strings, were lowered into holes drilled to a depth of 2450 m. The DOMs occupy the bottom 1000 m at intervals of 17 m where the glacial ice is transparent. In addition to the large scale array of optical sensors, the inner dense array called DeepCore was also deployed. Additional DOMs frozen into tanks located at the surface near the top of each hole constitute an air shower array called IceTop. IceTop provides us with the capability to study the atmospheric muon background reliably. The strings and tanks are arranged in a hexagonal

47 lattice pattern with a spacing of approximately 125 m. 97
 48 The array comprises 5160 DOMs on 86 strings of which 98
 49 8 strings corresponds to DeepCore, and 324 modules in 99
 50 the surface array. The DeepCore array was excluded 100
 51 in the current analysis. From June 2010 to May 2011, 101
 52 79 out of 86 strings were in operation. This run was 102
 53 followed by the initial year of data taken with the Ice- 103
 54 Cube full 86 string configuration that continued until 104
 55 May 2012. In this paper, results from the diffuse ultra- 105
 56 high energy (UHE) neutrino searches at PeV energies 106
 57 and higher with the 79 and full 86 string configurations 107
 58 of IceCube with data taken between 2010 and 2012 in 108
 59 total of 670.1 days of effective livetime are presented. 109

60 2. Analysis

61 2.1. Signals and backgrounds

62 Possible sources of astronomical neutrinos at PeV 114
 63 energies and higher include potential accelerators of 115
 64 cosmic-rays above 3×10^{15} eV (the “knee” of the 116
 65 cosmic-ray spectra), such as AGNs or GRBs. These 117
 66 cosmic-ray source models and the resultant neutrino 118
 67 fluxes have large uncertainties. Still, many models pre- 119
 68 dict signal neutrino spectra which follow a power-law. 120
 69 The spectral slope of the fluxes is predicted to be harder 121
 70 for cosmic neutrinos than that of background atmo- 122
 71 spheric muons and neutrinos. 123

72 In the energy region above 1 PeV, in addition to neu- 124
 73 trinos directly propagating from each source, there are 125
 74 highly expected secondary produced neutrinos in the 126
 75 propagation of the cosmic-rays. These “cosmogenic” 127
 76 neutrinos are produced in interactions of the highest 128
 77 energy cosmic-rays with the cosmic-microwave back- 129
 78 ground (CMB) and higher energy (infra-red, optical, 130
 79 and ultra violet) background [8, 9]. They may provide 131
 80 us a direct evidence of the highest energy cosmic-ray 132
 81 sources. This is because the spectral shapes and flux 133
 82 levels are sensitive to the redshift dependence of the 134
 83 cosmic-ray source distributions and cosmic-ray primary 135
 84 compositions [10]. The undeflected and unabsorbed na- 136
 85 ture of the neutrino propagation also give us an insight 137
 86 into their origin. The cosmic-ray fluxes and the CMB 138
 87 density are well measured, and thus secondary neutri- 139
 88 nos are guaranteed to exist due to well known photo- 140
 89 pion production mechanisms. The cosmogenic neutri- 141
 90 nos are distributed in a higher energy region than pos- 142
 91 sible background events. This makes the cosmogenic 143
 92 neutrino signal events less uncertain to be distinguished 144
 93 from background. 145

94 Most background events are induced by particles gen- 145
 95 erated in the interaction of cosmic-rays in the atmo- 146
 96 sphere. These atmospheric interactions produce two 147

97 types of background particles. One of these is muons 98
 99 with energies high enough to reach to at least the depth 100
 101 of 1.5 km in ice before losing all of their energy [11], 102
 103 and the other is atmospheric neutrinos. There is a great 104
 105 advantage in searches for neutrinos at PeV energies and 106
 107 higher also from the perspective of background reduc- 108
 109 tion. Since the conventional atmospheric neutrino and 109
 110 muon spectra are proportional to $E^{-3.7}$ or steeper, a very 110
 111 small number of background events is expected in the 111
 112 energy region. 112

113 In addition to those energy dependence, the atmo- 113
 114 spheric muon distribution has a strong zenith angle 114
 115 dependence. Because of the difference in the propa- 115
 116 gation distance, atmospheric muons peaks at verti- 116
 117 cal downward-going direction and sharply decrease to 117
 118 the horizontal direction. Atmospheric neutrinos have 118
 119 a weaker zenith angle dependence due to the interac- 119
 120 tion probability of neutrinos in the Earth. Because the 120
 121 neutrino-nucleon cross-section increases with energy, 121
 122 the Earth is transparent to neutrinos from all directions 122
 123 only up to PeV energies. At higher energies, the neu- 123
 124 trino mean free paths become significantly smaller than 124
 125 the Earth radius. At PeV energies and above, a neutrino 125
 126 distribution has a peak near the horizon. 126

127 When we refer to the atmospheric neutrinos, we as- 127
 128 sume the conventional atmospheric neutrinos unless ex- 128
 129 plicitly written. The conventional atmospheric neu- 129
 130 trinos come from decays of cosmic-ray induced pion 130
 131 and kaons in the atmosphere. At PeV energies and 131
 132 above, neutrinos from decays of charmed mesons are 132
 133 expected to dominate over the conventional atmospheric 133
 134 neutrinos, however. This contribution is called prompt 134
 135 atmospheric neutrinos. The energy at which prompt 135
 136 neutrinos begin to dominate is expected to be around 136
 137 3×10^5 GeV depending on models. The prompt atmo- 137
 138 spheric neutrino spectrum has a slope index of approx- 138
 139 imately -2.7, harder than that of conventional atmo- 139
 140 spheric neutrinos. The prompt atmospheric neutrino 140
 141 models involve highly uncertain charm meson produc- 141
 142 tion cross-section. While the perturbative-QCD calcu- 142
 143 lations [4] predict prompt neutrinos with theoretical un- 143
 144 certainty of a factor of two, non-perturbative part of 144
 145 QCD in the charm production involves a larger uncer- 145
 146 tainty. We have not observed clear evidence for prompt 146
 147 contributions in the atmospheric neutrinos so far [1]. 147

142 2.2. Event selections

143 Above PeV energies, the primary variable to dis- 143
 144 criminate signal from background is the energy of the 144
 145 particles. Because the amount of energy deposited by 145
 146 the neutrino-induced charged particles in the detector 146
 147 and observed as Cherenkov photons is highly correlated 147

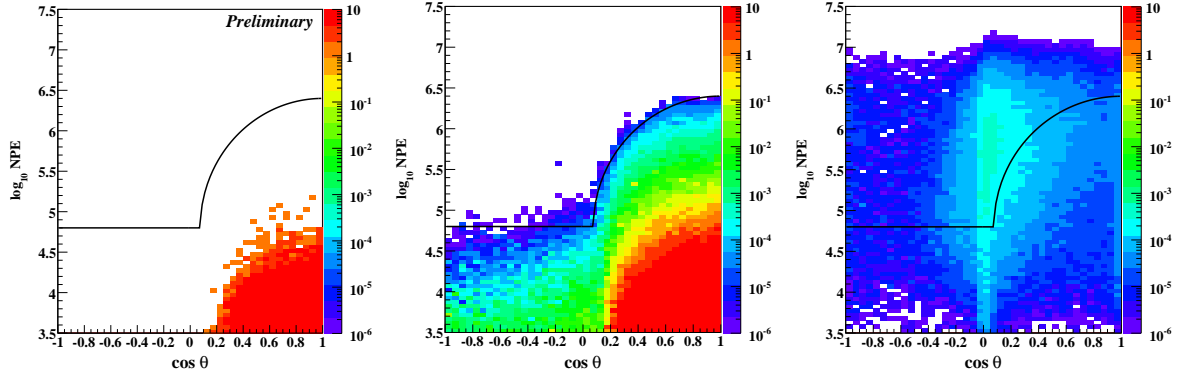


Figure 1: Event number distributions on the plane of NPE and reconstructed zenith angle in 498.4 hours are shown for the experimental 10% test sample from 2011-2012 (left panel), the total background (middle panel), and signal cosmogenic neutrino model [13] Monte Carlo simulations (right panel). The colors indicate event numbers per bin. The signal distributions are adding all three flavors of neutrinos. The background distributions include atmospheric muons from the CORSIKA package with SIBYLL high energy interaction model and conventional atmospheric neutrinos. The solid lines in each panel indicate the final selection criteria.

148 with their energy, the extremely-high energy neutrino
 149 signal stands out against the atmospheric muon and neu-
 150 trino background due to the much higher light depo-
 151 sition [7]. The total number of photo-electrons (NPE)
 152 recorded in a time interval of 11 μ s of an event is used
 153 as the main distinctive feature to separate signal from
 154 background after a lower level background reduction re-
 155 questing the number of hit DOMs greater than 300.

156 Then as the second step, we reconstruct the direc-
 157 tion of in-coming particles. Since the background atmo-
 158 spheric muons are concentrated in the direction of verti-
 159 cally downward-going while expected neutrino signals
 160 above PeV energies can only enter the IceCube detector
 161 from directions above slightly below the horizontal geo-
 162 metries, the final selection criterion was obtained as a
 163 reconstructed direction dependent NPE threshold value.

164 From May 31, 2010 to May 12, 2011, IceCube with
 165 79 strings was in operation, and the first year IceCube
 166 full configuration with 86 strings took data from May
 167 13, 2011 to May 15, 2012. The corresponding effec-
 168 tive livetimes for 2010-2011 and 2011-2012 runs are
 169 319.18 days and 350.91 days respectively excluding the
 170 period of detector calibration and unstable operation.
 171 Selection criteria are obtained by optimizing in each set
 172 of samples with different detector configurations using
 173 slightly different zenith angle reconstruction algorithms
 174 to minimize the model discovery factor [5, 6]. Presented
 175 here as an example is the selection criteria for the full
 176 string configuration run. The criteria for the 2010-2011
 177 data sample is quite similar but with slightly different
 178 values. The final selection criteria for 2011-2012 sam-
 179 ple are events with NPE exceeding the threshold values

as:

$$181 \log_{10} \text{NPE} \geq \begin{cases} 4.8 & \cos\theta \leq 0.075 \\ 4.8 + 1.6\sqrt{1 - (\frac{\cos\theta - 1.0}{0.925})^2} & \text{otherwise.} \end{cases} \quad (1)$$

182 In Fig. 1, the event number distributions of the Monte
 183 Carlo simulations and experimental data for 498.4 hours
 184 are shown. The period corresponds to the livetime of a
 185 10% test sample for the IceCube 2011-2012 configura-
 186 tion for examinations of the Monte Carlo simulations
 187 and detector responses. Following the blind analysis
 188 strategy, the signal selection criteria is obtained fully
 189 based on the Monte Carlo simulations of background
 190 and signal events. The solid lines in Fig. 1 indicates
 191 the final criteria (Eq. 1) for the sample.

192 The effective neutrino area of the analysis averaged
 193 over the approximately two years period with the dif-
 194 ferent IceCube detector configurations from June 2010
 195 to May 2012 is shown in Fig. 2. The effective areas
 196 are given for each neutrino flavor, averaged over
 197 4π solid angle. An equal flux of neutrinos and anti-
 198 neutrinos is assumed. The effective areas are approx-
 199 imately two times larger than for the 40 string confi-
 200 guration of data sampling period from 2008-2009 [5].
 201 The sharp peaked structure for electron neutrino effec-
 202 tive area corresponds to the Glashow resonance [12].

203 Below 5 PeV, the effective area of electron neutrinos
 204 exceeds that of muon or tau neutrinos. This reflects the
 205 fact that muon and tau tracks from muon/tau neutrinos
 206 partially deposit their energies into the detector volume
 207 while the electromagnetic (EM) cascades from electron
 208 neutrinos deposit 100% of their energy. While tracks
 209 have a longer propagation length, they do not satisfy the

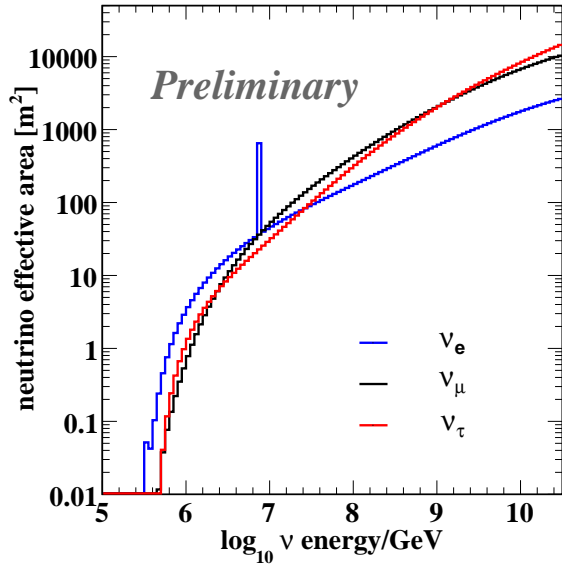


Figure 2: The IceCube neutrino effective area averaged over 670.1 days with different string configurations. Exposure of the sample used in this analysis is obtained by multiplying the effective area with the 670.1 days of livetime and 4π solid angle. The sharp peaked structure at 6.3 PeV for electron neutrino is due to the Glashow resonance [12].

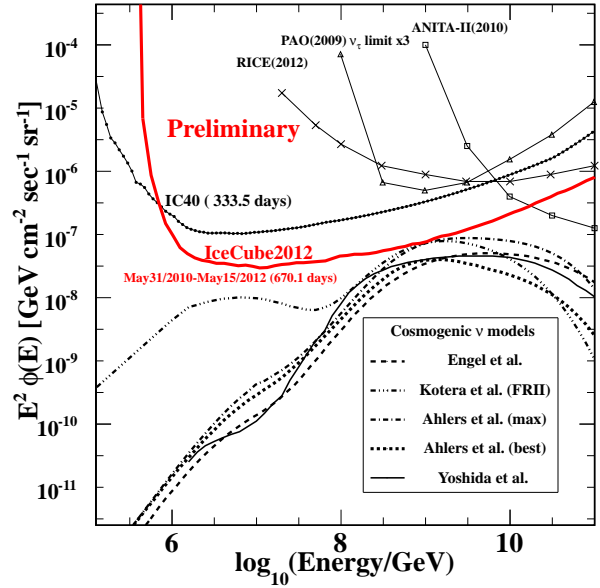


Figure 3: The IceCube differential sensitivity to all flavor neutrino flux by the 2010–2012 ultra-high energy neutrino analysis with an effective livetime of 670.1 days (red solid line). The systematic errors are not included. Several model predictions are shown for comparison: Engel et al. ($\Omega_\Lambda = 0.7$) [14], Kotera et al. (FRII) [15], Ahlers et al. (best and max) [16], Yoshida et al. ($(m, Z_{\max}) = (4, 4)$) [13]. Model fluxes are summed over all neutrino flavors, assuming standard neutrino oscillations. The model independent differential upper limits by other experiments are also shown for Auger (PAO) [17], RICE [18], ANITA [19], and the previous IceCube result (IC40) [5]. Limits from other experiments are converted to the all flavor limit assuming standard neutrino oscillation and a 90% quasi-differential limit per one energy decade when necessary.

210 selection criteria (Eq. 1) in the energy region, in contrast to
211 the EM cascades induced within detector.

212 The quasi-differential model-independent IceCube
213 sensitivity on neutrino fluxes using two years of Ice-
214 Cube data is shown in Fig. 3. The sensitivity is cal-
215 culated as in [20] requiring 2.44 events in a bin size of
216 one energy decade. The 2.44 is the Feldman-Cousins
217 up-fluctuation 90% CL limit event number for null ex-
218 pected events. The IceCube sensitivity to the neutrino
219 fluxes in the region between 1 PeV to 100 EeV from
220 previous study [5] is approximately a factor of four im-
221 proved. The factor of four improvement from previous
222 IceCube results is due to approximately a factor of two
223 longer livetime and a factor of two gain in the effective
224 area, while we are able to keep the similar background
225 event rates with the improved reconstruction algorithms
226 and Monte Carlo simulations.

227 3. Results

228 After unblinding of the full data sample with
229 670.1 days of effective livetime, we observe two signal
230 candidate neutrino events that pass all the selection cri-
231 teria. One event is from August 8th, 2011 with the NPE
232 value of 7.0×10^4 p.e. and 312 DOMs recorded photon

233 signal. The other event is from Jan 3rd, 2012 with the
234 NPE value of 9.6×10^4 p.e. and 354 DOMs recorded
235 photon signal.

236 The expected background event rate of atmospheric
237 muons and conventional atmospheric neutrinos is 0.057
238 events in the period. The background with prompt at-
239 mospheric neutrinos is 0.190 events assuming the stan-
240 dard prompt neutrino flux from Ref. [4]. Expected total
241 background numbers and each background contribution
242 are presented in Table 1. The preliminary p-value for the
243 background only hypothesis is calculated to be 1.6×10^{-3}
244 ($\sigma = 2.9$) and for the background with the nominal num-
245 ber of prompt atmospheric neutrinos [4] is 1.5×10^{-2} (σ
246 $= 2.2$).

247 An event display of the event from August 2011 is
248 shown in Fig. 4. Both events have a characteristic spher-
249 ical photon distribution. These distributions are consis-
250 tent with Cherenkov photons from particle cascades in-

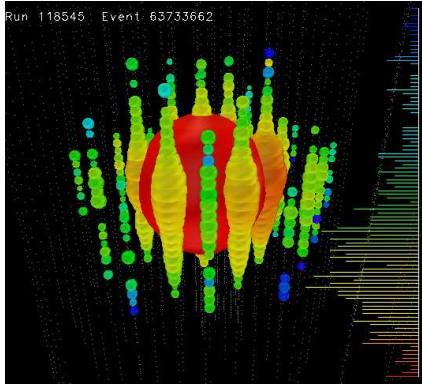


Figure 4: An event display of the one of the two observed events. Each spheres represent a DOM. Colors indicate the arrival timing of the photon (red = earliest, blue= latest). The size of the sphere indicates the measured photon in each DOM.

251 duced by neutrino interactions within the IceCube de-
 252 tector without outgoing muon or tau tracks. It is likely
 253 that these events are induced by either electron neutrinos
 254 of any interaction or neutral current interaction of
 255 muon or tau neutrinos. The preliminary total recon-
 256 structed energy deposits of these two cascade events are
 257 1.1 and 1.3 PeV with the reconstruction uncertainties
 258 of $\sim 35\%$ including statistical uncertainty and system-
 259 atic uncertainties associated with the ice properties and
 260 the absolute DOM sensitivity. These energy deposits
 261 correspond to the incoming neutrino energy if each cas-
 262 cade is the result of a charged current interaction of an
 263 electron neutrino where 100% of the neutrino energy is
 264 deposited near the interaction vertex. Including the hy-
 265 pothesis of neutral current interaction of three flavors of
 266 neutrinos, the statistical error, and the systematic error,
 267 the 90% most probable neutrino energies of two events
 268 at the earth surface correspond to 780 TeV-5.6 PeV and
 269 890 TeV-8.5 PeV, respectively, assuming that the sur-
 270 face neutrino flux follows an E^{-2} power law.

Background Contributions	Event Rates in 670 days
Atmospheric muons	0.036
Conventional atmospheric neutrinos	0.021
Total background	0.057
Total background with prompt ν [4]	0.190

Table 1: Preliminary number of background events in 670.1 days of effective livetime. Systematic uncertainties are not included. The magnitude of these uncertainties can be larger than the best-fit background expectation listed in the table.

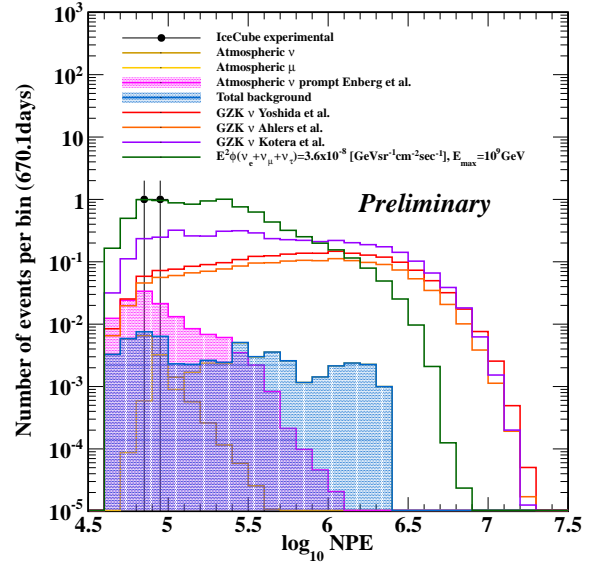


Figure 5: Event distributions from 2010-2012 sample passing the final selection criteria as function of $\log_{10} \text{NPE}$. Black marks indicate experimental data. Purple, red and orange solid lines indicate cosmogenic neutrino models with different assumed parameters. Green line indicates a power-law flux which follows E_{ν}^{-2} up to $E_{\nu} = 10^9$ GeV with the three flavor neutrino flux level of $E^2 \phi_{\nu_e + \nu_{\mu} + \nu_{\tau}} = 3.6 \times 10^8$ GeV $\text{sr}^{-1} \text{sec}^{-1} \text{cm}^{-2}$ corresponding to the obtained upper limit from the previous IceCube result in the similar energy range [5]. Filled magenta area is prompt atmospheric neutrino distribution and filled blue area is conventional atmospheric muon and neutrino background sum.

271 Figure 5 shows event distributions from two years of
 272 data passing the final selection criteria as a function of
 273 $\log_{10} \text{NPE}$ for experimental data, signal and background
 274 Monte Carlo simulations. Signal models include three
 275 cosmogenic neutrino models with different cosmic-ray
 276 source distributions or spectra. Among the three cosmo-
 277 genic neutrino models, the distribution from Ref. [15],
 278 with an assumption that cosmic-ray spectra at sources
 279 extend to lower energy than the other models, shows a
 280 better agreement compared to the other models, which
 281 produce neutrinos from interaction of UV/optical pho-
 282 tons. One of the signal models is an E^{-2} power-law
 283 neutrino flux which represent the contribution from di-
 284 rect neutrino production in cosmic-ray sources. The
 285 flux level corresponds to the upper limit obtained by
 286 the 2008-2009 IceCube data [5]. Table 2 presents the
 287 expected numbers of signal events from reference cos-
 288 mogenic neutrino models and experimentally observed
 289 numbers after the final selection. The numbers are given
 290 for the full energy region and the region above 100 PeV.
 291 Most of the cosmogenic neutrinos are neutrinos with en-
 292 ergies above 100 PeV. We would like to note that while

Cosmogenic ν Signal Models	Event Rates	
	All	$E_\nu \geq 100$ PeV
Yoshida et al. [13]	2.1	2.0
Kotera et al. (FRII) [15]	4.1	2.6
Ahlers et al. (maximal) [16]	3.2	3.0
Ahlers et al. (the best fit) [16]	1.6	1.5

IceCube Experimental	Event Rates	
	All	$E_\nu \geq 100$ PeV
May 31, 2010 - May 15, 2012	2	0

Table 2: Preliminary number of signal events from Monte Carlo simulations and experimentally observed events in 670.1 days of effective livetime at the final level of the analysis. Numbers are given for all the energy range and for the primary neutrino energy larger than 100 PeV. Errors are not included.

the cosmogenic neutrino models in the table predict 1.6~4.1 events in 670.1 days of an effective livetime, which is consistent as total rates with the experimental observation of two neutrino events, some of the models can be constrained with null observation of events above 100 PeV.

4. Summary

We presented the results of the analysis using the 2010-2012 data by the 79-string and 86-string IceCube detector to search for the ultra-high energy neutrinos with energies exceeding 10^6 GeV. The sensitivity of the analysis is improved by approximately a factor of four from the previous analysis [5]. Not including systematic uncertainties, the observation of 2 neutrino events corresponds to a 2.9 sigma excess above the event rates expected from atmospheric muons and conventional atmospheric neutrinos and 2.2 sigma excess with prompt atmospheric neutrinos. It is however possible that the significance of the excess may be reduced by the systematic uncertainties in the background estimate. The level of expected flux from the observation is consistent with the upper limit obtained by the previous UHE neutrino search [5], which is already below the Waxman-Bahcall limit [21].

References

- [1] G. Sullivan, in these proceedings.
[2] R. Abbasi *et al.* (IceCube Collaboration), Nucl. Instrum. Meth. **A618**, 139 (2010).
[3] R. Abbasi *et al.* (IceCube Collaboration), Nucl. Instrum. Meth. **A601**, 294 (2009).
[4] R. Enberg, M.H. Reno, and I. Sarcevic, Phys. Rev. D **78**, 043005 (2008).

- [5] R. Abbasi *et al.* (IceCube Collaboration), Phys. Rev. D **83**, 092003 (2011).
[6] G. C. Hill *et al.*, Statistical Problems in Particle Physics, Astrophysics, and Cosmology, In the Proceedings of PHYSTAT2005.
[7] R. Abbasi *et al.* (IceCube Collaboration), Phys. Rev. D **82**, 072003 (2010).
[8] K. Greisen, Phys. Rev. Lett. **16**, 748 (1966); G. T. Zatsepin and V. A. Kuzmin, Pisma Zh. Eksp. Teor. Fiz. **4**, 114 (1966) [JETP. Lett. **4**, 78 (1966)].
[9] V. S. Berezinsky and G. T. Zatsepin, Phys. Lett. **28B**, 423 (1969).
[10] S. Yoshida and A. Ishihara, Phys. Rev. D **85**, 063002 (2012).
[11] D. Chirkin and W. Rhode, arXiv:hep-ph/0407075v2.
[12] S. L. Glashow, Physical Review **118**, 316 (1960).
[13] S. Yoshida and M. Teshima, Prog. Theor. Phys. **89**, 833 (1993); The model with the source evolution $(z_{max} + 1)^m$ with $m = 4$ extending to $z_{max} = 4.0$.
[14] R. Engel, D. Seckel, and T. Stanev, Phys. Rev. D **64**, 093010 (2001).
[15] K. Kotera, D. Allard, and A. V. Olinto, J. Cosmol. Astropart. Phys. **10** 013 (2010).
[16] M. Ahlers, *et al.*, Astropart. Phys. **34**, 106 (2010).
[17] J. Abraham *et al.* (Pierre Auger Collaboration), Phys. Rev. D **79**, 102001 (2009). Private communications.
[18] I. Kravchenko *et al.* (Rice Collaboration), Phys. Rev. D **85**, 062004 (2012).
[19] P. W. Gorham *et al.* (ANITA Collaboration), Phys. Rev. D **82**, 022004 (2010); arXiv:1011.5004 (erratum).
[20] L. A. Anchordoqui *et al.*, Phys. Rev. D **66**, 103002 (2002).
[21] E. Waxman and J. Bahcall, Phys. Rev. D **59**, 023002 (1999); S. Razzaque, P. Meszaros, and E. Waxman. Phys. Rev. D, **68** 083001 (2003).